Sustainable Chemical Engineering
https://ojs.wiserpub.com/index.php/SCE/

UNIVERSAL WISER PUBLISHER

Research Article

Synergistic Effect of Magnetic Composites on Zirconia Mineral for the Reduction of Eminent Pb (II) and Cd (II) from Synthetic Wastewater

Hema Avrilia[1], Agustiya Nuraini[1], Chairul Irawan[1*], Iryanti Fatyasari Nata[1], Meilana Dharma Putra[1], Primata Mardina[1], Rinny Jelita[1], Muhammad Al Muttaqii[2]

[1]Department of Chemical Engineering, Lambung Mangkurat University, Banjarbaru, South Kalimantan, 70714, Indonesia
[2]Research Center for Chemistry, National Research and Innovation Agency (BRIN), B.J. Habibie Science and Technology Area, South Tangerang, 15314, Indonesia
E-mail: cirawan@ulm.ac.id

Received: 8 July 2025; **Revised:** 8 September 2025; **Accepted:** 10 September 2025

Abstract: Water contamination by heavy metals represents a critical global environmental challenge, necessitating the development of efficient and sustainable treatment solutions. The significant potential of Zirconia (ZrO_2) as a high-quality adsorbent remains underdeveloped, particularly in Indonesia, for water treatment and purification applications. This is especially relevant given the growing environmental concern over heavy metal contamination in water supplies. This research aims to address this by developing zirconia-based magnetic particles for use as an efficient adsorbent. Zirconia-coated magnetic particles (Fe_3O_4@ZrO_2) were synthesized via chemical co-precipitation. The adsorbent was then characterized using Scanning Electron Microscopy (SEM), Energy-Dispersive X-ray spectroscopy (EDX), X-Ray Diffraction (XRD), and Fourier Transform Infrared Spectroscopy (FTIR), which confirmed that modifying ZrO_2 with Fe_3O_4 altered its structure, creating particles with a greater surface area ideal for adsorption. Subsequent adsorption tests for Pb (II) and Cd (II) demonstrated excellent removal capabilities, with maximum adsorption capacities of 189.21 mg/g and 85.22 mg/g, respectively. The combination of ZrO_2 adsorption properties with the magnetic characteristics of Fe_3O_4 shows great promise for applications in water treatment and wastewater management, offering a potential method for reducing heavy metal pollutants.

***Keywords*:** adsorption, Fe_3O_4@ZrO_2, heavy metal, magnetic particles, wastewater treatment

1. Introduction

Human activities, particularly industrial operations and mining, have significantly increased the levels of heavy metals such as arsenic, cadmium, lead, and mercury in water bodies. These elements are not only pervasive but also persist in ecosystems, accumulating in soils and water and ultimately entering the food chain, where they pose serious health risks to both aquatic life and humans. This environmental pollution, in turn, negatively affects the water ecosystem and poses health risks to humans who consume contaminated organisms. As released by the World Health Organization (WHO), heavy metals are the most harmful water pollution for human health. They can be strongly toxic by mixed with different environmental elements, such as water, soil, and air where humans and other living organisms can be exposed to them through the food chain.[1] Owing to their toxicity, the contamination of heavy

DOI: https://doi.org/10.37256/sce.6220257127

metals in water has become a major environmental concern. Some of the growing industries in Indonesia, such as battery plants, smelters, pigment/plastic additive factories, and e-waste wastewater, contain high amounts of inorganic pollutants such as Pb (II) and Cd (II). The levels of their concentrations fluctuate between 5 and 20 mg/L,[2] surpassing the legal limits of 0.05 mg/L for Pb and 0.005 mg/L for Cd established by Indonesian government law.

In Indonesia, zirconia minerals are mostly found as alluvial deposits on land, oceans, coastal areas and river. They are often found alongside other minerals such as cassiterite and electrum, including gold and silver, while their associated minerals include ilmenite, magnetite, monazite, xenotime, pyrite, sulfides, and silica.[3] Zirconia minerals are economically found in a granular form as result of the weathering of acidic igneous and metamorphic rocks that are then transported, concentrated and deposited with cassiterite, rutile, ilmenite, pyrite, magnetite, gold, and iron oxides. Beyond their geological significance, zirconia-based materials are prized in numerous high-tech and industrial realms, including electrocatalysis, energy devices, coatings for optical elements, ceramic biomaterials, Ultraviolet (UV) sensors, electronics, and dielectric and nanocomposite applications.[4]

Recently, zirconia has garnered attention in water treatment research. Notably, a critical review indicates that zirconium-based adsorbents (like zirconium oxides and impregnated complexes) show excellent capacity to remove harmful ions, such as copper, lead, arsenic, fluoride, and phosphate through mechanisms like ligand exchange, surface complexation, Lewis acid-base interactions, and electrostatic attraction, then this is challenging to utilizing various synthesis methods to produce ZrO_2-based nanostructures with varied physicochemical characteristics.[5] Yuan et al.,[6] synthesized the zirconium-based adsorbent using the sol-gel method, resulting in a distinctive nanostructured morphology characterized by low crystallinity and a high density of active hydroxyl groups, demonstrating significant potential for various applications. In 2025, Drużyński, et al.,[7] synthesized micrometer-sized binary ZrO_2@SiO_2 with the sol-gel method and this study found that the capacity for adsorption and release in the synthesized material was strongly determined by the number of surface functional groups and the porosity of the material. Unlike other recent studies, the zirconium composite produced through the sol-gel method, which generated MgO@ZrO_2 oxide material, showed remarkable adsorption properties, largely due to the wide surface area of the material. Another research employed graphene oxide templates in the fabrication of nano-zero-iron-reduced-zero graphite oxide composites as well as hydrated zirconium-oxide nanocomposites, taking advantage of the GO templates' superior mechanical strength and large surface area.[8,9]

Zirconia, known for its radiation tolerance and compatibility with metal and other materials, is a promising inert matrix candidate. Hydrous zirconia hydrogels have been demonstrated to effectively bind heavy metals, showing promising adsorption behavior for water decontamination.[10] It is chemically inert with acidic and basic active centers, as well as oxidation and reduction sites on its surface, making it seen as a potential adsorbent and photocatalyst for ions in view of its high affinity, for instance, efficiently removing heavy metals via both adsorption and photocatalytic oxidation.[11-13] Previous studies indicated that magnetic nanomaterials can partially compensate for heavy metals removal due to their easy phase separation after treatment. Among various nano-magnetic materials, Fe_3O_4 is the most common and widely utilized because it can quickly achieve magnetic separation when exposed to an external magnetic field.[14,15]

Fe_3O_4 nanoparticles, however, exhibit limited adsorption capacity and chemical stability, which restricts their use in heavy metal ion contamination remediation. Certain published research highlights the importance of surface modification of magnetic nanoparticles in boosting their stability and adsorption properties.[3,9,16,17] Thus, zirconia's potential as an inert matrix motivates the need for this study with an aim of modifying zirconia with magnetic nanoparticle material due to its properties.

The synthesis of nanomagnetite (Fe_3O_4) has been widely done using various methods, such as co-precipitation, hydrothermal, thermal decomposition, and sol-gel technique. Co-precipitation here is the most commonly used synthesis method to produce magnetic nanoparticles under low temperature, allowing for the easy control of particle size, resulting in a relatively short processing time.[15] The recent study of zirconia magnetic nanoparticles composites has utilized the co-precipitation synthesis method, applying them as magnetic adsorbents, which successfully removed any unhealthy materials from wastewater,[18] and it was found that Fe_3O_4@ZrO_2 nanocomposite is a promising nanocomposite for industrial waste during wastewater treatment. Nevertheless, additional research could investigate surface modification techniques or the incorporation of composite materials to enhance the adsorbent adsorption efficiency. Furthermore, exploring the use of the adsorbent for removing other pollutants is a promising area for future research. Hence, this research aims to synthesize the magnetite particles using the co-precipitation method. This approach aims to develop zircon oxide composites with magnetic particles capable of being utilized in drinking water treatment and

assisting in the remediation of industrial or domestic wastewater containing a range of ions and dissolved substances. Therefore, this study proposes the co-precipitation synthesis of an Fe_3O_4@ZrO_2 composite designed for drinking water treatment and industrial/domestic wastewater remediation. It aims to harness magnetic separation, zirconia adsorption strength, and novel active interfacial properties to improve heavy metal removal while addressing stability and retrieval challenges in real-wastewater treatment applications. In this work, a novel Fe_3O_4@ZrO_2 composite was synthesized via the co-precipitation method. This promising material, with its unique interface, can create new active sites, alter the surface charge, enhance stability (by preventing Fe_3O_4 oxidation and leaching), and potentially lead to cooperative adsorption mechanisms.

2. Methods

2.1 *The synthesis of zircon oxide with magnetic particles composites*

The zirconia minerals were collected from Katingan in Central Kalimantan, Indonesia. Iron (III) chloride hexahydrate ($FeCl_3 \cdot 6H_2O$), iron (II) sulfate heptahydrate ($FeSO_4 \cdot 7H_2O$), lead (II) nitrate ($Pb(NO_3)_2$), cadmium (II) nitrate ($Cd(NO_3)_2$), hydrochloric acid (HCl), and sodium hydroxide (NaOH) were obtained from Thermo Scientific ACROS. All chemicals used were of analytical grade and did not undergo any additional purification treatment.

The process of chemical co-precipitation was employed to produce magnetic particles on zircon oxide. It was initiated by preparing the solution of $FeSO_4 \cdot 7H_2O$, $FeCl_3 \cdot 6H_2O$, and zircon mineral by dissolving the components in distilled water at a molar ratio of 1.33 : 2.66 : 1, referred to as the precursor solution. The mixture underwent titration by adding 5 M NaOH until an equilibrium pH of 6 was achieved. The mixture was then left to precipitate at 60 °C for 48 hours to form a solid product. The precipitated solid was washed extensively with distilled water to clear away any residual chemicals. To simplify the separation process, a magnet was utilized during washing to isolate the composite from the mixture. Subsequently, the purified product was dried at 105 °C in an oven for 12 hours. After the drying process, it was processed with a mortar and pestle until it could pass through a 100-mesh sieve. The final product, Fe_3O_4@ZrO_2, was stored in a sealed container for future applications.

2.2 *The batch adsorption process of Pb (II) and Cd (II) solutions*

The adsorption process was conducted through a batch experiment by contacting zirconia composites with 100 mL artificial solution samples containing 100 mg/L of Pb (II) and Cd (II) ions. 0.1 gram of composite was added to each sample and placed in a shaker at a speed of 150 rpm. It was conducted by shaking at ambient temperatures at the contact time of 5-240 minutes; variation of pH from 3 to 11; and varying process temperatures between 25 and 60 °C. The solution was separated at the end of the experiment through the application of an external magnetic field. Furthermore, atomic adsorption spectroscopy (PerkinElmer 2100 Atomic Absorption Spectrometer) analysis was conducted to assess the residual metal content in the filtrate. The metal ion adsorption was quantified based on the difference between the initial and equilibrium concentrations of the adsorbate. The adsorption studies here were performed in triplicate to ensure the accuracy of the mean values calculated from the data obtained. The Sigma Plot® software, version 14, was used for the analysis and presentation of the experimental results in a graphical format.

3. Results and discussion

3.1 *Characterization of Fe_3O_4@ZrO_2 composites*

The chemical composition, morphology, and structure of zirconia mineral and Fe_3O_4@ZrO_2 composites were examined through Scanning Electron Microscopy with Energy Dispersive X-ray Spectroscopy (SEM ZEISS EVO 10). Figure 1a shows the Scanning Electron Microscopy (SEM) images illustrating the smooth surface characteristic of ZrO_2 in a representative sample. The Fe_3O_4@ZrO_2 composites showed magnetic particles formed on the zirconia surface layer, appearing as irregular amorphous agglomerates. Figure 1b visualizes the magnetite particles distributed on the modified ZrO_2 that served as the primary matrix. Figure 1d presents SEM-Energy Dispersive X-Ray Spectroscopy

(SEM-EDS) analysis identified the presence of Fe, Zr, C, and O elements within the magnetic composite particles of Fe_3O_4@ZrO_2. The Fe_3O_4 particles prepared by the co-precipitating process are smaller along ZrO_2 and more densely distributed, implying that these composites likely possess a higher affinity to adsorb the Pb (II) and Cd (II) ions. The magnetic ions in the composite adsorbent allow for rapid, easy separation with a magnet. The synergistic effect yields higher capacity for Pb/Cd than individual components, and then the stable core-shell structure enables regeneration and multiple reuse cycles.

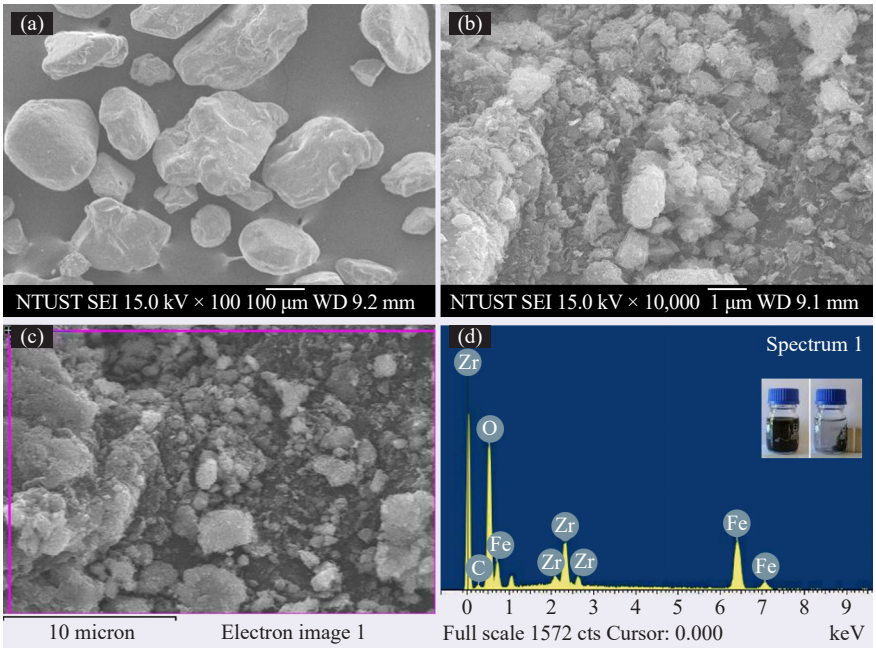

Figure 1. SEM images of (a) Mineral ZrO_2 (b) Magnetic particles at Zircon Oxide (Fe_3O_4@ZrO_2) (c) Scattering area for EDS of Magnetic particles at Zircon Oxide (Fe_3O_4@ZrO_2), and (d) EDS images of Magnetic particles at Zircon Oxide (Fe_3O_4@ZrO_2)

Table 1 presents the diffraction components contained in the composite. EDS data showed total amount of chemical composition of composites revealing that the composite was primarily composed by Fe and Zr, providing the evidence of magnetite and zirconia mineral as major component in the sample.

Table 1. Compositions of Fe_3O_4@ZrO_2 composites measured by SEM-EDS

No	Component	Percentage of Mass, %
1	C	2.02
2	O	19.64
3	Fe	52.23
4	Zr	26.11
Total		100.00

Figure 2 depicts X-Ray Diffraction (XRD) analysis (XRD Bruker D8 Advance) conducted to identify the crystallinity of mineral ZrO_2 (before synthesis) and Fe_3O_4@ZrO_2 composites. The diffraction pattern of Fe_3O_4@

ZrO_2 showed several slightly broader peaks, reflecting distortions in the ZrO_2 crystal structure, which is typically characterized by sharp and narrow peaks. The ZrO_2 pattern weakened and shifted due to the diffusion of Fe ions into the ZrO_2 lattice during the synthesis process, forming a composite layer that modified its crystal structure. The diffraction pattern of the Fe_3O_4@ZrO_2 composite was observed at 2 theta values of 30.14°, 35.49°, 43.28°, and 57.2° with planes (220), (311), (400), and (511), respectively, indicating the cubic spinel structure of Fe_3O_4 (JCPDS Card No. 001-1111), which confirmed the presence of the magnetite phase in the composite.[19]

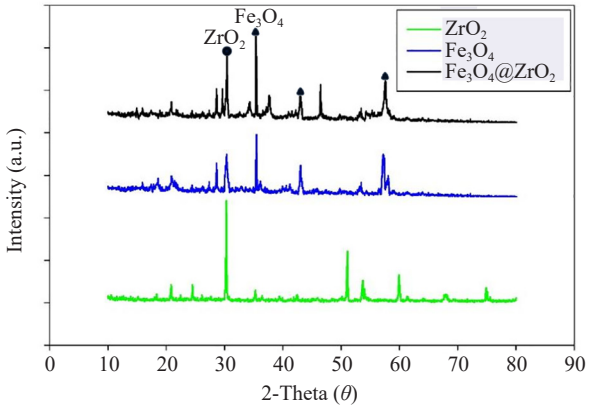

Figure 2. The typical XRD structural characteristic of zirconia (ZrO_2), magnetite (Fe_3O_4), and magnetic particles at zirconia mineral (Fe_3O_4@ZrO_2)

Table 2 shows a higher crystallinity index of ZrO_2 compared to Fe_3O_4 and the Fe_3O_4@ZrO_2 composite. Subsequently, the crystallinity index of ZrO_2 significantly decreased from 99.74% to 47.50% after the synthesis process into the Fe_3O_4@ZrO_2 magnetic particle composite, indicating that the crystallinity of pure ZrO_2 material was greater than that of the Fe_3O_4@ZrO_2 composite. After the synthesis process, the crystallinity of ZrO_2 material tended to decrease as Fe_3O_4 modified the crystal lattice of ZrO_2.[20] Fe_3O_4 had a lower crystallinity in view of its complex spinel crystal structure, with the distribution of Fe^{2+} and Fe^{3+} cations causing imperfections in the crystal geometry. This is confirmed by characterization results from ref. 21,[21] showing that ZrO_2 has small crystallite sizes and a more stable structure, whereas Fe_3O_4 has more crystal defects and larger crystallite sizes. This aspect relates to the surface area, which can present more active sites on the adsorbent, leading to a higher likelihood of interaction with the adsorbate and consequently greater adsorption capacity. The crystallinity index obtained from XRD readings aligns with previous studies,[13] indicating that Fe_3O_4 tended to be more amorphous when being composited with ZrO_2, thereby affecting the total crystallinity of the composite material.

Table 2. Crystallinity of ZrO_2, Fe_3O_4, and Fe_3O_4@ZrO_2

Sample	Crystalinity index (%)
ZrO_2	99.74%
Fe_3O_4	26.33%
Fe_3O_4@ZrO_2	47.50%

Based on the Fourier Transform Infrared Spectroscopy (FTIR) spectrum of the original ZrO_2 and Fe_3O_4@ZrO_2 composite (Figure 3), functional groups were identified based on the observed peaks, as in the wavelength range of 3,000-3,500 cm^{-1}, a broad hydroxyl (O-H) peak was detected, indicating water or moisture adsorption from the

surrounding environment by the material surface. Furthermore, peaks within the wavelength range of 1,400-1,650 cm^{-1} were attributed to the elongation of O-H groups, suggesting the presence of adsorbed moisture within the material.[13] In the FTIR spectrum of $Fe_3O_4@ZrO_2$, a sharp peak around 500-600 cm^{-1} corresponds to the Fe-O bond. Peaks appearing in the range of 500-850 cm^{-1} indicate the presence of Zr-O bonds, a characteristic feature of zirconia.[22]

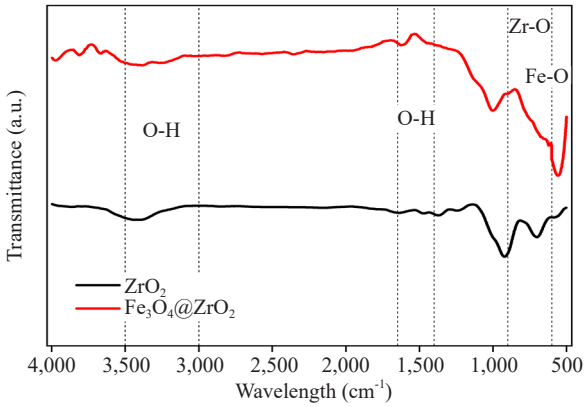

Figure 3. FTIR spectrum analysis for zirconia (ZrO_2) and magnetic particles at zirconia mineral ($Fe_3O_4@ZrO_2$)

3.2 *Batch adsorption*

The batch adsorption process for Pb (II) and Cd (II) was performed with different contact durations within the range of 5 to 480 minutes, pH range of 3 to 9 and temperature range of ambient, 40 °C, and 60 °C in an artificial solution of Pb (II) and Cd $(II)^+$ ions. Contact time, pH, and temperature of the adsorption process were carried out using the $Fe_3O_4@ZrO_2$ composites to obtain the optimum conditions, which were observed by their adsorption capacity, measuring their adsorption performance. The experimental results can be seen in Figure 4-6, respectively.

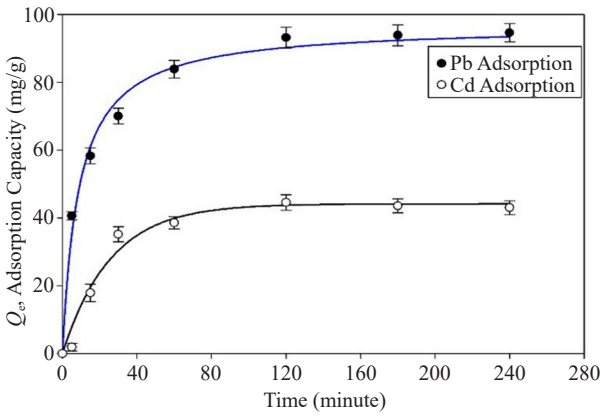

Figure 4. The capacity for adsorbing Pb (II) and Cd (II) ions was measured at different contact times with $Fe_3O_4@ZrO_2$ as the adsorbent. Conditions for the experiment included 1 g/L adsorbent, stirring at 150 rpm, for consistency: ambient temperature and a pH of 7.0 ± 0.2

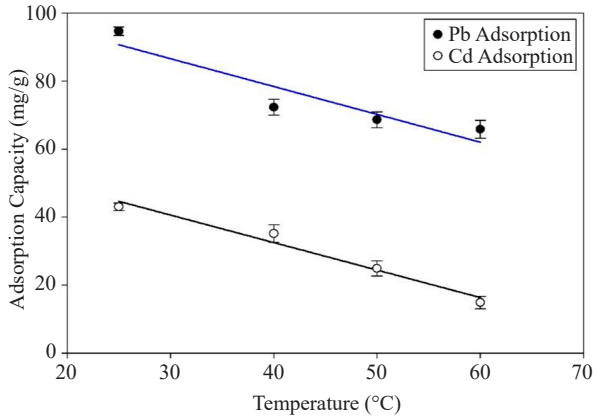

Figure 5. The capacity for adsorbing Pb (II) and Cd (II) ions was measured at different temperatures with Fe_3O_4@ZrO_2 as the adsorbent. Conditions for the experiment included 1 g/L adsorbent, stirring at 150 rpm, contact time of 4 h, and a pH of 7.0 ± 0.2

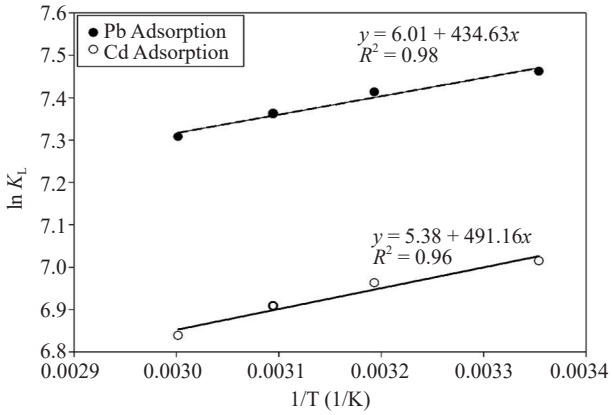

Figure 6. Van't Hoff plot for adsorbing Pb (II) and Cd (II) ions was measured at different temperatures with Fe_3O_4@ZrO_2 as the adsorbent. Conditions for the experiment included 1 g/L adsorbent, stirring at 150 rpm, contact time of 4 h, and a pH of 7.0 ± 0.2

3.2.1 *Kinetic study on the adsorption of Pb (II) and Cd (II)*

The adsorption behavior of Pb (II) and Cd (II) by Fe_3O_4@ZrO_2 composite was analyzed in relation to contact time under ambient conditions and pH 7.0 ± 0.2. The operating parameters specified an initial concentration of 100 mg/L for both Pb (II) and Cd (II), with an adsorbent dosage of 1 g/L and a stirring rate of 150 rpm. Figure 4 indicates that within the first 30 minutes, the adsorption capacity of Pb rose sharply to 70.039 mg/g as a result of diffusion into the pores and surface of the adsorbent, which still contained numerous free active sites.[23] Later, the increase in adsorption capacity became less significant until it became constant. The adsorption equilibrium of Pb (II) and Cd (II) was finally achieved at 96.614 mg/g and 43.014 mg/g sequentially, within 240 minutes (4 h). The effect of initial pH and temperature was examined at an optimal contact time of 4 h for the subsequent Pb (II) and Cd (II) adsorption study.

The adsorption study based on the kinetic model was described using a pseudo second order model, which employed the following equation:[24]

$$Q_t = \frac{t \times k_1 \times Q_e^2}{1 + (t \times Q_e \times k_1)} \quad (1)$$

where Q_e (mg/g) indicates the quantity of Pb (II)/Cd (II) ions adsorbed at equilibrium and Q_t (mg/g) represent the quantity of Pb (II)/Cd (II) ions at time t, and k_1 (mg/(g·min)) is the rate constant of pseudo second order model. Using non-linear regression, the parameter values and correlation coefficients were determined and summarized in Table 3.

Table 3. Kinetic parameters of Pb (II) and Cd (II) adsorption onto the Fe_3O_4@ZrO_2 at ambient temperature

Kinetic model	Metal adsorbed	
Pseudo second order	Pb (II)	Cd (II)
Q_e (mg/g)	96.891	44.150
k_1 (mg/(g·min))	1.2×10^{-3}	3.9×10^{-2}
R^2	0.990	0.971
$\sum \Delta q$	0.379	0.192

The pseudo second order kinetics model describes the adsorption process for Pb (II) and Cd (II) ions using data fitted for both adsorbents, with R^2 values of 0.990 and 0.971, respectively. Applying this kinetic model typically suggests that the reaction rates might be approximated.

3.2.2 *Effect of temperature and thermodynamic studies on the adsorption of Pb (II) and Cd (II)*

The influence of temperature serves as a crucial diagnostic method to differentiate between physisorption and chemisorption. Figure 5 shows that the temperature elevation led to a decrease in adsorption capacity. According to ref. 25,[25] the binding forces between the adsorbate and adsorbent weaken as the temperature increases, leading to a reduction in adsorption capacity.

The drastic decline in adsorption capacity from room temperature to 40 °C suggests that the adsorption of Pb (II) and Cd (II) ions becomes more favorable at lower ambient temperature to 60 °C. In a previous study by ref. 23,[23] the desorption of metal ions was observed, indicating the weak van der Waals interactions between the metal ions and the adsorbent surface are observed after heating, that a phenomenon known as physisorption. Thus, the optimum temperature for the Fe_3O_4@ZrO_2 composite to adsorb Pb (II) and Cd (II) ions is at ambient temperature (23 ± 2 °C).

In thermodynamic studies, the amounts of adsorbed Pb (II) and Cd (II) ions at 25-60 °C were measured to determine the thermodynamic parameters: the standard Gibbs free energy change ($\Delta G°$), the standard enthalpy change ($\Delta H°$), and the standard entropy change ($\Delta S°$).

The standard Gibbs free energy change for the adsorption process is related to the Langmuir equilibrium constant, K_L, by the following equation:

$$\Delta G° = - RT \ln (K_L) \quad (2)$$

where R is the universal gas constant (8.314 J/mol·K) and T is the absolute temperature in Kelvin.

The standard enthalpy change ($\Delta H°$) and standard entropy change ($\Delta S°$) were determined from the van't Hoff equation:

$$\ln (K_L) = -(\Delta H°/R)(1/T) + (\Delta S°/R) \quad (3)$$

A van't Hoff plot of ln (K_L) versus $1/T$ yielded a linear relationship (Figure 6). The slope of the line is equal to $-\Delta H°/R$ and the intercept is equal to $\Delta S°/R$. The calculated thermodynamic parameters are presented in Table 4.

The negative value of $\Delta H°$ confirms that the adsorption process was exothermic and favored at lower temperatures. The negative values of $\Delta G°$ indicate that the adsorption of Pb (II) and Cd (II) onto Fe_3O_4@ZrO_2 was spontaneous. The positive value of $\Delta S°$ indicates an increase in randomness at the solid-liquid interface during adsorption, which reflects a high affinity of the adsorbent for Pb (II) and Cd (II) ions. The low magnitude of $\Delta H°$ of -3.61 and -4.08 kJ/mol for Pb (II) and Cd (II), respectively, is characteristic of physisorption, as it falls within the typical range for physical adsorption processes (5-40 kJ/mol).[3,26-28] This value, indicating unspecific adsorption, is consistent with a mechanism driven primarily by electrostatic interactions and van der Waals forces.

Table 4. Thermodynamic parameters for Pb (II) and Cd (II) adsorption onto the Fe_3O_4@ZrO_2

T (K)	$1/T$	K_L (L/mol)		ln K_L		$\Delta G°$ (kJ/mol)		$\Delta H°$ (kJ/mol)		$\Delta S°$ (J/mol·K)	
		Pb (II)	Cd (II)	Pb (II)	Cd (II)	Pb (II)	Cd (II)	Pb (II)	Cd (II)	Pb (II)	Cd (II)
298.15	0.0033	1,740.48	1,112.90	7.4619	7.0147	-18.50	-17.39				
313.15	0.0032	1,657.60	1,056.69	7.4131	6.9628	-19.30	-18.13	-3.61	-4.08	49.97	44.73
323.15	0.0031	1,574.72	1,000.48	7.3618	6.9082	-19.78	-18.56				
333.15	0.0030	1,491.84	933.04	7.3077	6.8384	-20.24	-18.94				

3.2.3 *The effect of initial pH on the adsorption of Pb (II) and Cd (II)*

The initial pH is not merely a controllable parameter but a key element that determines the essential electrostatic forces involved in adsorption. The effect mainly influences the chemistry of both the adsorbent and the adsorbate. Figure 7 demonstrate a remarkable increase in adsorption capacity from lower to higher pH due to the protonation of the Fe_3O_4@ZrO_2 composite at low pH, leading to a positively charged adsorbent surface, which reduced affinity towards positively charged ions.

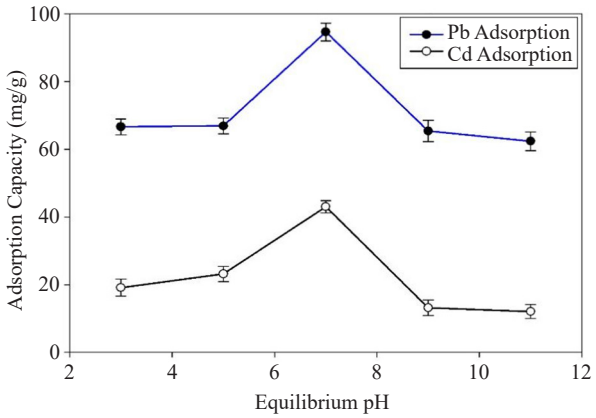

Figure 7. The capacity for adsorbing Pb (II) and Cd (II) ions was measured at different pH with Fe_3O_4@ZrO_2 as the adsorbent. Conditions for the experiment included 1 g/L adsorbent, stirring at 150 rpm, contact time of 4 h, and ambient temperature

The low adsorption capacity for Pb (II) and Cd (II) at low pH is attributed to greater competition between metal ions and H^+ ions for the active sites of the Fe_3O_4@ZrO_2 composite.[29] At low pH, the functional groups on the surface of Fe_3O_4@ZrO_2 are mostly associated with H^+ ions by reason of repulsive forces, as the adsorbed metal ions have positive charges. Surprisingly, adsorption capacity decreased at pH 9, indicating that excessively high pH can also hinder adsorption owing to deprotonation on the composite surface, reducing its electrostatic interaction with metal ions. A significant difference in adsorption capacity between Pb (II) and Cd (II) ions across various parameters is associated with the adsorption capacity of the two metals being related to their ionic radius (22). Lead, Pb (II), compared to Cd (II), has a larger ionic radius, resulting in relatively weaker electrostatic forces and a weaker ability to attract water molecules around it. On account of this weak water attraction, the hydration radius of Pb (II) is getting smaller, and its movement in water is faster, making Pb (II) more easily accessible to the adsorbent surface.

3.2.4 *Adsorption isotherm studies on the adsorption of Pb (II) and Cd (II)*

Using the Langmuir isotherm, the adsorption behavior was assessed under the assumption that monolayer adsorption happens when molecules adsorb onto the surface, creating a saturated layer, with a constant number of

available adsorption sites. The Langmuir equation is presented as follows:[30]

$$Q_e = \frac{K_L Q_{max} C_o}{1 + K_L C_o} \quad (4)$$

where Q_e represent the equilibrium of Pb (II)/Cd (II) on the adsorbent (mg/g); C_o denotes to the initial concentration of Pb (II)/Cd (II) in solution (mg/L); Q_{max} indicates the monolayer capacity of the adsorbent (mg/g); and K_L represent the Langmuir constant.

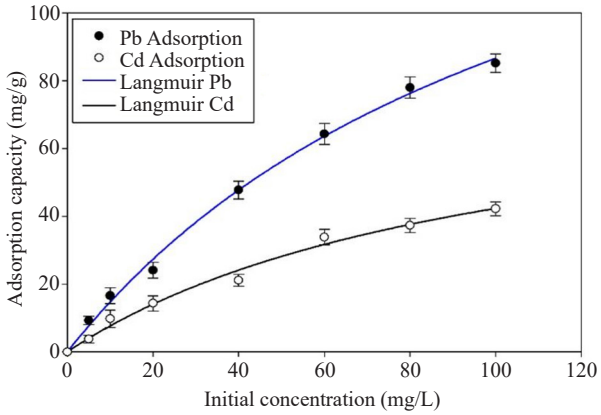

Figure 8. Adsorption capacity of Pb (II) and Cd (II) ions at different initial concentrations, with ambient temperature, pH of 7 ± 0.2, contact time of 4 h, 1 g/L adsorbent, and stirring at150 rpm

Table 5. The adsorption capacity of Pb (II) and Cd (II) observed on various adsorbents

Adsorbent	Adsorption capacity (mg/g)		pH	Reference
	Pb (II)	Cd (II)		
Zeolite-supported Nanoscale Zero-Valent Iron (Z-NZVI)	85.37	48.63	6	33
$KMnO_4$-treated Magnetic Biochar (FMBC)	148	79	> 2.5	34
Magnetic-Biochar	58.65	42.48	6	35
Zr-BAD	60.76	53.59	7	28
Fe_3O_4@ZrO_2	189.21	85.22	7	This study

According to Figure 8, the adsorption density escalated with the rise in Pb (II)/Cd (II) concentration. The increased concentration meant that more metal ions were in solution, allowing for greater absorption. The adsorbed amount of adsorbate in the adsorbent shows a direct linear relationship with the increasing concentration.[3,31,32] According to this research, similar to other studies, higher concentrations enhance the interaction between adsorbate and adsorbent molecules during adsorption. Therefore, it may enhance the likelihood of adsorption. These findings also support Langmuir models, which suggest that the amount of substances adsorbed is proportional to the applied pressure or concentration. The Langmuir model satisfactorily described the adsorption data (average R^2 value = 0.99) and the maximum batch adsorption capacities for Pb (II) and Cd (II) were found to be 189.21 mg/g and 85.22 mg/g using Fe_3O_4@ZrO_2 as adsorbent, respectively.

A comparison was made between the adsorption capacity of another adsorbent to assess its effectiveness. The

adsorption capacities of different Fe/magnetic particle-containing adsorbents are displayed in Table 5. It was found that the performance of Fe_3O_4@ZrO_2, Fe_3O_4@ZrO_2 compared to other adsorbents, was much better in terms of adsorption capacity towards the Pb (II) and Cd (II) ions.

3.2.5 *Assessment of the reusability and stability of the adsorbent in Pb (II) and Cd (II) adsorption*

An investigation into the reusability capacity and stability of the Fe_3O_4@ZrO_2 adsorbent revealed its strong potential for repeated use in Pb (II) and Cd (II) ions removal. The regeneration process, involving magnetic separation and desorption with 0.01 M HCl (3), successfully stripped approximately 93% of the adsorbed ions by displacing them with hydrogen ions at low pH. Although a slight reduction in performance was observed after four cycles, as shown in Figure 9, with adsorption capacities falling to 6.62% and 11.1%, respectively for Pb (II) and Cd (II) adsorption, this is consistent with other magnetic composites. The decline is due to permanent changes in surface functional groups and incomplete desorption, which reduce available active sites and weaken electrostatic interactions.[3,8,31] Reduced adsorption capacity was related to the incomplete desorption of divalent metal ions on the adsorbent surface. This finding demonstrated that Fe_3O_4@ZrO_2 was suitable as a reusable adsorbent.

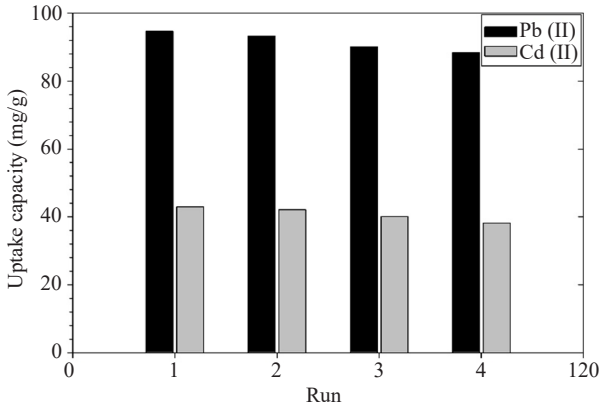

Figure 9. Repetition of Pb (II) and Cd (II) ions adsorption onto Fe_3O_4@ZrO_2 at ambient temperature, pH of 7 ± 0.2, contact time of 4 h, 1 g/L adsorbent, and stirring at150 rpm

Furthermore, this composite Fe_3O_4@ZrO_2 particle approach was found to be very easy to synthesize, cost effective, and environmentally benign, and applicable in large-scale adsorption processes for wastewater treatment. The combination of zirconia and magnetic particles composite in considering their abilities as adsorbent, becomes a solution for wastewater issues. The limited capacity of zirconia to adsorb metal ion pollutants can be overcome by magnetic particles, which have magnetic properties. In brief, the Fe_3O_4@ZrO_2 composite, with its high specific surface area from ZrO_2 and the magnetic properties of Fe_3O_4 that are able to attract metal ions, makes it excellent as an adsorbent.

4. Conclusions

Magnetic particles at zirconia (Fe_3O_4@ZrO_2) were successfully produced by a chemical co-precipitation process and analyzed through characterizations using SEM-EDS, XRD, and FTIR, while their magnetizations and removal abilities were examined within batch adsorption in the artificial solution of 100 mg/L Pb (II) and Cd (II) ions. The optimum adsorption capacity of Fe_3O_4@ZrO_2 composite for Pb (II) and Cd (II) ions at 189.21 mg/g dan 85.22 mg/g, respectively in batch adsorption process at ambient temperature, pH of 7 ± 0.2, contact time of 4 h, 1 g/L adsorbent, and stirring at 150 rpm using Langmuir adsorption model, indicated that Fe_3O_4@ZrO_2 is an effective adsorbent in the reducing of metal ions in the solution. The combination of ZrO_2 adsorption properties and Fe_3O_4 magnetic characteristics has shown great potential for application in water treatment and wastewater management with further development. The other

advantages of this Fe_3O_4@ZrO_2 composites are the magnetic iron oxide (magnetite) provides the magnetic properties that are easy to retrieve in the solution, zirconium dioxide has a high affinity for heavy metals like Pb (II) and Cd (II), while the Fe_3O_4@ZrO_2 is quite stable and regenerated using low acidic acid.

Acknowledgments

This research was financially supported by a grant from the Directorate of Research and Community Service, the Ministry of Higher Education, Science and Technology, Republic of Indonesia, the fund for Excellence Research University Grant (Contract Number: 1382/UN8.2/PG/2025).

Conflict of interest

The authors declared that they have no known competing financial interests or personal relationships that could appear to have influenced the work reported in this paper.

References

[1] Mitra, S.; Chakraborty, A. J.; Tareq, A. M.; Emran, T. B.; Nainu, F.; Khusro, A.; Simal-Gandara, J. Impact of heavy metals on the environment and human health: Novel therapeutic insights to counter the toxicity. *J. King Saud Univ. Sci.* **2022,** *34*(3), 101865.

[2] Kurniawan, T. A.; Liang, X.; Singh, D.; Othman, M. H. D.; Goh, H. H.; Gikas, P.; Shoqeir, J. A. Harnessing landfill gas (LFG) for electricity: A strategy to mitigate greenhouse gas (GHG) emissions in jakarta (Indonesia). *J. Environ. Manage.* **2022,** *301*, 113882.

[3] Irawan, C.; Refki, M. F.; Hidayat, R.; Mu'minah, R.; Nata, I. F.; Putra, M. D.; Triantoro, A. Synthesis of magnetic nanoparticles coated zirconia using one-pot solvothermal processes as adsorbent for Pb (II) and Cd (II) removal. *S. Afr. J. Chem. Eng.* **2023,** *45*, 247-255.

[4] Routray, S.; Mohanty, R.; Swain, R.; Sahu, S.; Mishra, B. R. Preparation and characterisation of zirconia nanomaterials prepared from zircon minerals of Brahmagiri coast. *J. Inst. Eng. (India): Ser. E* **2021,** *102*(1), 87-95.

[5] Zhao, D.; Yang, Y.; Chen, J. P. Performance of removing aqueous contaminant by zirconium-based adsorbents: A critical review. *Front. Chem. Eng.* **2024,** *6*, 1282076.

[6] Yuan, B.; Wu, P.; Liu, C.; He, J.; Jiang, W. Highly effective adsorption of As (III) and As (V) via zirconium-based materials with abundant active groups and capacity. *Chem. Eng. J.* **2025,** *511*, 161948.

[7] Drużyński, S.; Mazurek, K.; Kiełkowska, U.; Ciesielczyk, F.; Jesionowski, T. Adsorption of Cu (II) and Zn (II) onto ZrO_2-SiO_2 composite: Characteristics, mechanism and application in wastewater treatment. *Desalination Water Treat.* **2024,** *320*, 100657.

[8] Fan, X.; Ma, L.; Liu, S.; Xie, Y.; Lu, S.; Tan, Z.; Hu, Y. B. Facile synthesis of lattice-defective and recyclable zirconium hydroxide-coated nanoscale zero-valent iron for robust arsenite removal. *Sep. Purif. Technol.* **2022,** *302*, 122085.

[9] Wang, Q.; Zhu, S.; Xi, C.; Zhang, F. A review: Adsorption and removal of heavy metals based on polyamide-amines composites. *Front. Chem.* **2022,** *10*, 814643.

[10] Yang, J.; Chu, Y.; Li, Z.; Zhang, Y. Effective removal of heavy metals by nanosized hydrous zirconia composite hydrogel and adsorption behavior study. *Environ. Sci. Pollut. Res.* **2018,** *25*(33), 33464-33477.

[11] Gugushe, A. S.; Mpupa, A.; Munonde, T. S.; Nyaba, L.; Nomngongo, P. N. Adsorptive removal of Cd, Cu, Ni and Mn from environmental samples using Fe_3O_4-ZrO_2@APS nanocomposite: Kinetic and equilibrium isotherm studies. *Molecules* **2021,** *26*(11), 3209.

[12] Li, J.; Su, J.; Wang, Y.; Yang, Z.; Yang, Q. Efficient removal of hexavalent chromium by a novel magnetic zirconium-iron composite oxide (MZIO) from aqueous solution: Kinetic, isotherm, and mechanism. *Colloids Surf. A* **2022,** *641*, 128440.

[13] Zare, M. H.; Mehrabani-Zeinabad, A. Photocatalytic activity of ZrO_2/TiO_2/Fe_3O_4 ternary nanocomposite for the degradation of naproxen: Characterization and optimization using response surface methodology. *Sci. Rep.* **2022,**

12(1), 10388.
[14] Bhogal, S.; Sharma, R. Harnessing magnetic nanoparticles for cleaner water: A green technology perspective. *Sustain. Chem. One World* **2025,** *7*, 100083.
[15] Srivastava, A.; Katiyar, A. Zinc oxide nanostructures. In *Ceramic Science and Engineering*; Misra, K. P.; Misra, R. D. K., Eds.; Elsevier: Amsterdam, 2022; pp 235-262.
[16] Irawan, C.; Nata, I. F.; Putra, M. D. Synthesis of magnetic zirconium oxide-iron oxide nanoparticles composite using chemical precipitation process for Pb (II) adsorption. *Chem. Eng. Commun.* **2025,** *212*(5), 683-694.
[17] Zhang, X.; Xue, Y.; Gao, J.; He, C.; Ji, Y.; Dou, Y. Comparison of adsorption mechanisms for cadmium removal by modified zeolites and sands coated with Zn-layered double hydroxides. *Chem. Eng. J.* **2020,** *380*, 122578.
[18] Goudarzi, M. G.; Bagherzadeh, M.; Taheri, F.; Rostami-Vartooni, A. Preparation and characterization of magnetic zirconium oxide nanocomposite as a catalyst for reduction of methylene blue. *SN Appl. Sci.* **2020,** *2*(7), 1249.
[19] Davar, F.; Majedi, A.; Abbasi, A. Synthesis of Fe_3O_4@ZrO_2 core-shell nanoparticles through new approach and its solar light photocatalyst application. *J. Mater. Sci.: Mater. Electron.* **2017,** *28*(6), 4871-4878.
[20] Bashir, M.; Riaz, S.; Naseem, S. Fe_3O_4-stabilized zirconia: Structural, mechanical and optical properties. *J. Sol-Gel Sci. Technol.* **2015,** *74*(2), 281-289.
[21] Dontsova, T.; Kyrii, S.; Yanushevska, O.; Suprunchuk, V.; Kosogina, I. Physicochemical properties of TiO_2, ZrO_2, Fe_3O_4 nanocrystalline adsorbents and photocatalysts. *Chem. Pap.* **2022,** *76*(12), 7667-7683.
[22] Riahi, F.; Bagherzadeh, M.; Hadizadeh, Z. J. R. A. Modification of Fe_3O_4 superparamagnetic nanoparticles with zirconium oxide; preparation, characterization and its application toward fluoride removal. *RSC Adv.* **2015,** *5*(88), 72058-72068.
[23] Devi, B.; Goswami, M.; Rabha, S.; Kalita, S.; Sarma, H. P.; Devi, A. Efficacious sorption capacities for Pb (II) from contaminated water: A comparative study using biowaste and its activated carbon as potential adsorbents. *ACS Omega* **2023,** *8*(17), 15141-15151.
[24] Anangadan, S. M.; Pradhan, S.; Saththasivam, J.; McKay, G.; Mackey, H. R. A kinetic evaluation of nutrient and organic matter removal in greywater for green walls: Assessing the performance of Mineral-Based, Organic, and Waste-Derived plant support media. *Sep. Purif. Technol.* **2024,** *349*, 127517.
[25] Jedli, H.; Almonnef, M.; Rabhi, R.; Mbarek, M.; Abdessalem, J.; Slimi, K. Activated carbon as an adsorbent for CO_2 capture: Adsorption, kinetics, and RSM modeling. *ACS Omega* **2024,** *9*(2), 2080-2087.
[26] Do, D. D. *Adsorption Analysis: Equilibria and Kinetics*; Academic Press: San Diego, CA, 1998.
[27] Lian, J. J.; Wu, M.; Wu, H. Y.; Liu, Y. T.; Xu, Q.; Miao, M. J.; Li, X. L. Enhanced molybdenum (VI) adsorption by zirconia sol-modified nanoscale iron sulfide: Performance, mechanism and influencing factors. *Desalination Water Treat.* **2023,** *299*, 137-153.
[28] Mubarak, A. S.; Salih, S. S.; Kadhom, M.; Ghosh, T. K. Competitive and non-competitive adsorption of Cd (II) and Pb (II) from aqueous solution using Zr-BADS metal-organic frameworks. *Sustain. Chem. Environ.* **2025,** *9*, 100231.
[29] Cruz-Lopes, L. P.; Macena, M.; Esteves, B.; Guiné, R. P. Ideal pH for the adsorption of metal ions Cr^{6+}, Ni^{2+}, Pb^{2+} in aqueous solution with different adsorbent materials. *Open Agric.* **2021,** *6*(1), 115-123.
[30] Langmuir, I. The adsorption of gases on plane surfaces of glass, mica, and platinum. *J. Am. Chem. Soc.* **1918,** *40*(9), 1361-1403.
[31] Batool, F.; Mohyuddin, A.; Amjad, A.; Ul Hassan, A.; Nadeem, S.; Javed, M.; Kurniawan, T. A. Removal of Cd (II) and Pb (II) from synthetic wastewater using *Rosa damascena* waste as a biosorbent: An insight into adsorption mechanisms, kinetics, and thermodynamic studies. *Chem. Eng. Sci.* **2023,** *280*, 119072.
[32] El-Wakeel, S. T.; Fathy, N. A.; Tawfik, M. E. Porous carbons prepared from a novel hard-wood composite waste for effective adsorption of Pb (II) and Cd (II) ions. *RSC Adv.* **2023,** *13*(49), 34935-34946.
[33] Li, Z.; Wang, L.; Meng, J.; Liu, X.; Xu, J.; Wang, F.; Brookes, P. Zeolite-supported nanoscale zero-valent iron: New findings on simultaneous adsorption of Cd (II), Pb (II), and As (III) in aqueous solution and soil. *J. Hazard. Mater.* **2018,** *344*, 1-11.
[34] Sun, C.; Chen, T.; Huang, Q.; Wang, J.; Lu, S.; Yan, J. Enhanced adsorption for Pb (II) and Cd (II) of magnetic rice husk biochar by $KMnO_4$ modification. *Environ. Sci. Pollut. Res.* **2019,** *26*(9), 8902-8913.
[35] Huang, F.; Zhang, S. M.; Wu, R. R.; Zhang, L.; Wang, P.; Xiao, R. B. Magnetic biochars have lower adsorption but higher separation effectiveness for Cd^{2+} from aqueous solution compared to nonmagnetic biochars. *Environ. Pollut.* **2021,** *275*, 116485.